Brief Communications

Temporal Control of Rac in Schwann Cell–Axon Interaction Is Disrupted in *NF2*-Mutant Schwannoma Cells

Yoko Nakai,[1] Yi Zheng,[1] Mia MacCollin,[2] and Nancy Ratner[1]

[1]Division of Experimental Hematology, Cincinnati Children's Hospital Research Foundation, Department of Pediatrics, University of Cincinnati, Cincinnati, Ohio 45229, and [2]Department of Neurology, Neurogenetics, Massachusetts General Hospital East, Charlestown, Massachusetts 02129

Schwann cell–axon interaction is the hallmark feature of peripheral nerves, yet the intracellular signals underlying this interaction are unknown. Schwann cells extend processes and migrate on developing axons before differentiation, requiring coordinated regulation of the Schwann cell cytoskeleton. Small GTPases of the Rho family, including Rho, Rac, and cell division cycle 42, regulate the actin cytoskeleton. The neurofibromatosis type 2 (*NF2*) gene is commonly mutated in schwannomas, Schwann cell tumors that contain cells lacking axon interaction. NF2 is involved in suppression of Rac signaling, and cultured schwannoma cells contain elevated, GTP-bound, active Rac. Despite these previous studies, a causal relationship between Rac activation and the abnormal cellular morphology of schwannoma is unknown. We used fluorescence resonance energy transfer to follow Rac activity in normal human Schwann cells and schwannoma cells during interaction with neurons. Normal Schwann cells elongated processes along neurites under low Rac activity. Schwannoma cells showed high Rac activity at distal regions of the cells and failed to align processes with neurites. Application of a Rac-specific inhibitor, the chemical compound NSC23766, to schwannoma cells restored neuronal interaction. The data support the significance of regulated Rac signaling in mediating Schwann cell–axon interaction and suggest that controlling Rac activity as a possible therapy for schwannomas.

Key words: Schwann cell; Rac; NF2; axon; live-cell imaging; FRET

Introduction

Schwann cells are the myelin-forming cells of the peripheral nervous system. Normal Schwann cells approach each other and induce changes in axons; a set of reciprocal interactions between Schwann cells and axons results in the complex morphology of the node and paranode of the differentiated myelin-forming Schwann cells (Vabnick et al., 1996). Establishment of Schwann cell polarity involves the regulation of actin cytoskeleton (Fernandez-Valle et al., 1997).

Neurofibromatosis type 2 (*NF2*) gene mutation leads to Schwann cell tumors, schwannomas, that arise from the nerve sheath. Schwannomas are benign tumors containing Schwann cells that fail to interact with axons. In primary culture, schwannoma cells show disorganized cytoskeleton structure such as spread areas fivefold to sevenfold greater than normal Schwann cells, aberrant membrane ruffling, and numerous, disorganized stress fibers (Pelton et al., 1998; Bashour et al., 2002).

Small-GTPases of the Rho family [Rho, Rac, and cell division cycle 42 (Cdc42)] regulate the actin cytoskeleton (Hall, 1998). Schwannoma cells have increased active Rac and its downstream effector p21-activated kinase (PAK) (Kaempchen et al., 2003). NF2 is involved in suppression of Rac-PAK signaling by blocking the p21 binding domain (PBD) of PAK (Kissil et al., 2003) or by binding to Rho-GDI, a GDP dissociation inhibitor, that may stabilize the inactive form of Rac (Maeda et al., 1999). Loss of NF2 alters Rac-PAK-mediated proliferation (Xiao et al., 2005), migration (Shaw et al., 2001), and contact inhibition (Okada et al., 2005). Despite the evidence placing NF2 into the Rac pathway, the function of Rac in normal Schwann cells and its relevance to Schwann cell tumor formation are yet to be answered.

In this work, we show that deregulated Rac causes cellular defects characteristic of human schwannomas. Using fluorescence resonance energy transfer (FRET), we followed the Rac activity in Schwann and schwannoma cells over time of interaction with neurons. In normal Schwann cells, Rac was highly active at the initial contact and rapidly became inactive during neuronal interaction, whereas in schwannoma cells, it was continuously active. Suppression of Rac before contact with neurons restored neuronal interaction to schwannoma cells. The data indicate that regulation of Rac is required at early time point for successful Schwann cell–neuron interaction and suggest that suppression of Rac as a possible therapy for schwannomas.

Materials and Methods

Cell culture. Normal human nerve Schwann cells were a kind gift from Dr. P. Wood (University of Miami, Miami, FL) provided through the Life Alliance Organ Recovery Agency of the University of Miami Miller School of Medicine. Human Schwann cells and schwannoma cells were

Received Nov. 11, 2005; revised Feb. 9, 2006; accepted Feb. 13, 2006.

This work was supported by National Institutes of Health Grant CA75824 (W.I., N.R.). We thank Dr. Michiyuki Matsuda for providing the FRET probes and Drs. Yi Rao and Michael Ward (Northwestern University, Chicago, IL) for the technical guidance for FRET. We thank Drs. Patrick Wood and Linda White (University of Miami, Miami, FL) for the generous gift of normal human nerve Schwann cells. We also thank Dr. Linda Parysek (University of Cincinnati, Cincinnati, OH) for the anti-neurofilament-15g1 antibody. We appreciate the participants in the alignment assay (J.J., M.D., X.S., W.N., L.W., W.C., and W.L.). We thank Dr. Wallace Ip (University of Cincinnati, Cincinnati, OH) for generous support.

Correspondence should be addressed to Yoko Nakai, Division of Experimental Hematology, Cincinnati Children's Hospital Research Foundation, 3333 Burnet Avenue, Cincinnati, OH 45229. E-mail: yoko.nakai@cchmc.org.

DOI:10.1523/JNEUROSCI.4865-05.2006

 0270-6474/06/263390-06$15.00/0

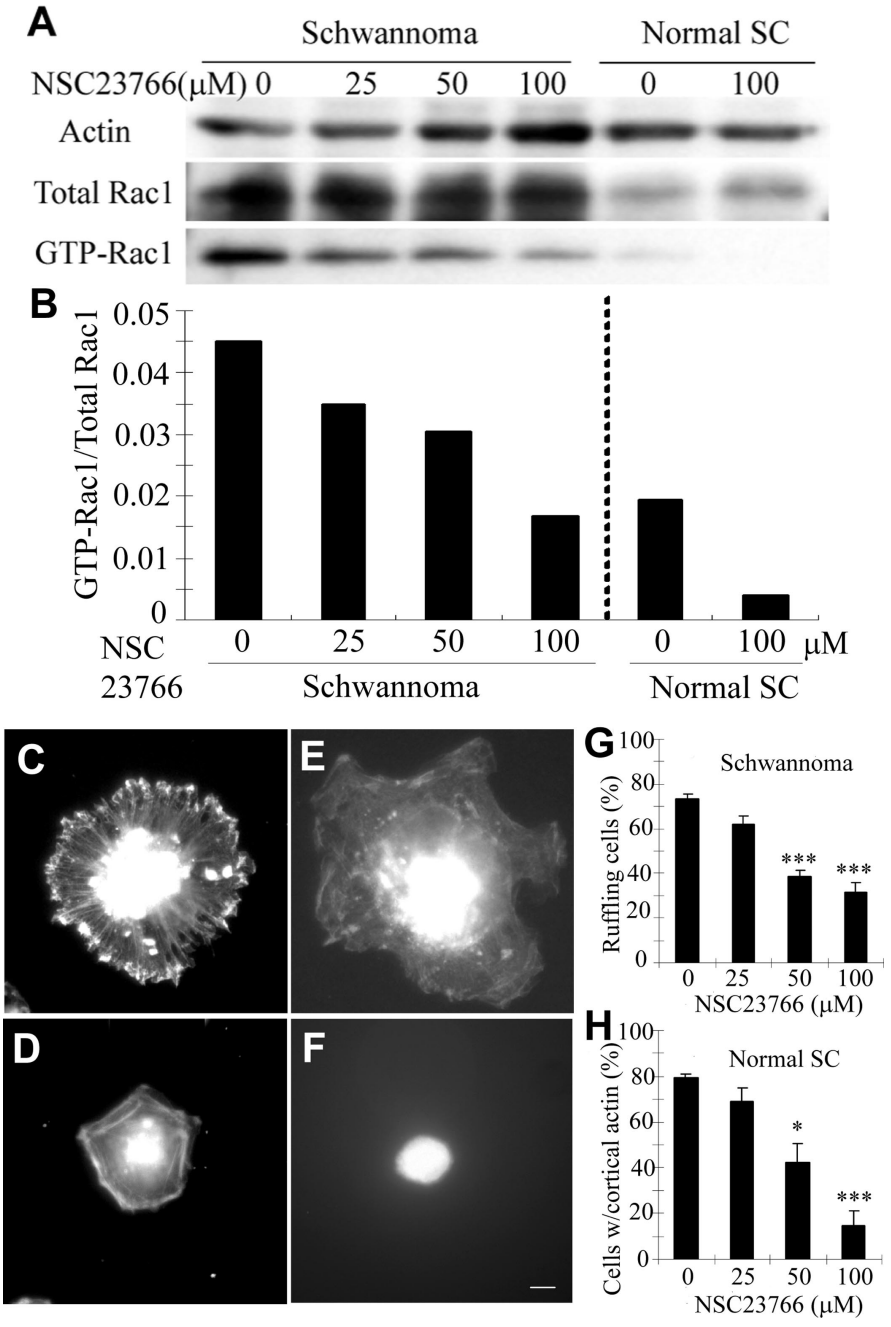

Figure 1. GTP-Rac in Schwann cells and schwannoma cells is suppressed by NSC23766. ***A***, PAK1-PBD pull-down of schwannoma cells and normal Schwann cells (SC), both pretreated with the indicated concentrations of NSC23766, were blotted with anti-Rac1 antibody. ***B***, Quantification of GTP-Rac1 normalized by total Rac1 showed higher Rac1 activity in schwannoma cells compared with normal Schwann cells (SC), which was suppressed by NSC23766 in a dose-dependant manner. ***C–H***, Schwann/schwannoma cells pretreated with NSC23766 were subjected to ruffling assay (see Materials and Methods). Membrane ruffling characteristic in schwannoma cells (***C***) but not in normal Schwann cells (***D***) was suppressed by NSC23766 treatment (***E***). Percentage of schwannoma cells with actin accumulation on the edge was quantified (***G***). In normal Schwann cells, membrane spreading was suppressed by the same treatment (***F***). Percentage of normal Schwann cells (SC) with a rim of cortical actin was quantified (***H***). Images are representative of a panel of cells in each condition. Scale bar: ***C–F***, 10 μm. Error bars represent mean ± SD ($n = 3$) (***G***, ***H***). *$p < 0.01$, ***$p < 0.001$ (Student's *t* test).

cultured as described previously (Bashour et al., 2002). Dorsal root ganglia (DRG) neurons from embryonic day 17 rats were enzymatically dissociated and plated on a collagen-coated cover glass, followed by 1 μM cytosine arabinoside treatment for 2 d. A neurite network substrate for Schwann cell–neuron coculture was established after 4 d of culture.

Rac pull-down assay. Schwann/schwannoma cells cultured at 80% confluency in the presence of 10% serum were pretreated with a chemical compound, NSC23766, in cell suspension at 37°C for 2 h. Cell lysates were incubated with PAK1-PBD agarose beads (Upstate, Charlottesville, VA) according to the protocol of the manufacturer and blotted with anti-Rac1 antibody (1:250 dilution; BD Transduction Laboratories, Franklin Lakes, NJ) or anti-actin antibody (1:1000 dilution; Cell Signaling Technology, Beverly, MA). The intensity of blots was measured by NIH ImageJ 1.34.

Ruffling assay. Schwann/schwannoma cells were pretreated with NSC23766 as above, plated on a laminin-coated cover glass for 20 min, and stimulated with serum for 30 min. Cells were fixed with 4% paraformaldehyde, permeabilized with 0.1% Triton X-100, and double labeled with anti-S100 antibody (1:500 dilution; DakoCytomattion, High Wycombe, UK) and phalloidin (Sigma, St. Louis, MO) (supplemental Figs. 1, 2, available at www.jneurosci.org as supplemental material). For each sample, 100 of S100-positive cells were counted.

Schwann cell–DRG neurite alignment assay. Schwann/schwannoma cells prelabeled with Cell Tracker green 5-chloromethyl fluorescein diacetate (Invitrogen, Carlsbad, CA) were pretreated with or without 100 μM NSC23766 as above. Cells were seeded onto rat DRG neuron cultures, and, 3 h later, 0 or 100 μM NSC23766 was added. After 24 h incubation, cells were fixed, permeabilized, and stained with anti-neurofilament-15g1 antibody (Parysek and Goldman, 1987). Deconvolved images of *z* stacks were created by Volocity 3.5.1 software (Improvision, Lexington, MA). For quantification, seven views, which contained 10–50 Schwann/schwannoma cells in each, were scored by seven observers who were not informed of the condition. Schwann/schwannoma cells with a process longer than the cell body aligning with the neurites were scored as aligned.

FRET analyses. Recombinant adenovirus plasmids of pAdeno-Raichu-Rac1–1011x and pAdeno-Raichu-RhoA-1237x were kind gifts from Dr. M. Matsuda (Osaka University, Osaka, Japan). CsCl-purified adenovirus probes were infected to Schwann/schwannoma cells at the multiplicity of infection of 50. Cells were used after 36–48 h of infection. In some experiments, 100 μM NSC23766 was added. The microscope stage was heated at 37°C in a live cell incubator (In Vivo Technologies, St. Louis, MO). Cyan fluorescent protein (CFP) and yellow fluorescent protein (YFP) images were acquired with an OI-05-Ex excitation filter (436 ± 20 nm; Chroma Technology, Brattleboro, VT) and OI-05-Em emission filters (480 ± 30 nm for CFP and 535 ± 40 nm for YFP; Chroma Technology). After background subtraction, YFP/CFP ratio images were created with Openlab 4.0.3 software (Improvision).

Results

GTP-Rac is suppressed by NSC23766, a Rac-specific inhibitor

We applied NSC23766, a small-molecule Rac-specific inhibitor (Gao et al., 2004), to primary cultures of human Schwann cells or to primary schwannoma cells isolated from patient tumors. First,

we defined the efficiency of NSC23766. GTP-Rac was monitored by pull-down assay. NSC23766 inhibited GTP-Rac1 in both cell types (Fig. 1*A*) in a dose-dependent manner (Fig. 1*B*). At 100 μM NSC23766, the relative Rac1 activity in schwannoma cells became close to that of normal Schwann cells (Fig. 1*B*). The amount of GTP-Cdc42, a closely related small GTPase, was not affected (data not shown), confirming the specificity of NSC23766 Rac inhibitor (Gao et al., 2004). As reported previously (Kaempchen et al., 2003), both activation and expression of Rac1 were significantly higher in schwannoma cells than in normal Schwann cells (Fig. 1*A*). The expression of total Rac1 normalized to actin was 2.24 ± 0.29 and 0.80 ± 0.07 in schwannoma cells and normal Schwann cells, respectively. Even normalized to the altered expression levels, the basal level of GTP-Rac1 was two times higher in schwannoma cells than in normal Schwann cells (Fig. 1*B*, 0 μM).

Rac plays a pivotal role in membrane ruffling (Ridley et al., 1992). Membrane ruffling is a characteristic feature of schwannoma cells, which can be suppressed by dominant-negative Rac, or reconstitution of the NF2 protein (Pelton et al., 1998; Bashour et al., 2002). Phalloidin staining of schwannoma cells showed typical membrane ruffling, with actin accumulation on the edge (Fig. 1*C*), absent in normal Schwann cells (Fig. 1*D*). Although it did not normalize the aberrant large size of schwannoma cells (Pelton et al., 1998), pretreatment with NSC23766 effectively suppressed their membrane ruffling (Fig. 1*E*). The same treatment also altered the morphology of normal Schwann cells, which became rounded (Fig. 1*F*). This effect was reversible; when Schwann cells pretreated with NSC23766 were transferred to medium without the drug, at 3 h, the cells remained rounded, but, within 24 h, all cells were attached to the dish with normal morphology and without significant reduction in cell number (data not shown). The effects of NSC23766 on suppression of membrane ruffling in schwannoma cells (Fig. 1*G*) and inhibition of membrane spreading in normal Schwann cells (Fig. 1*H*) were both dose dependent. Because both overactivation (Fig. 1*C*) and oversuppression (Fig. 1*F*) of Rac affect the morphology of Schwann cells, it appears that precise regulation of Rac is required to maintain normal Schwann cell morphology.

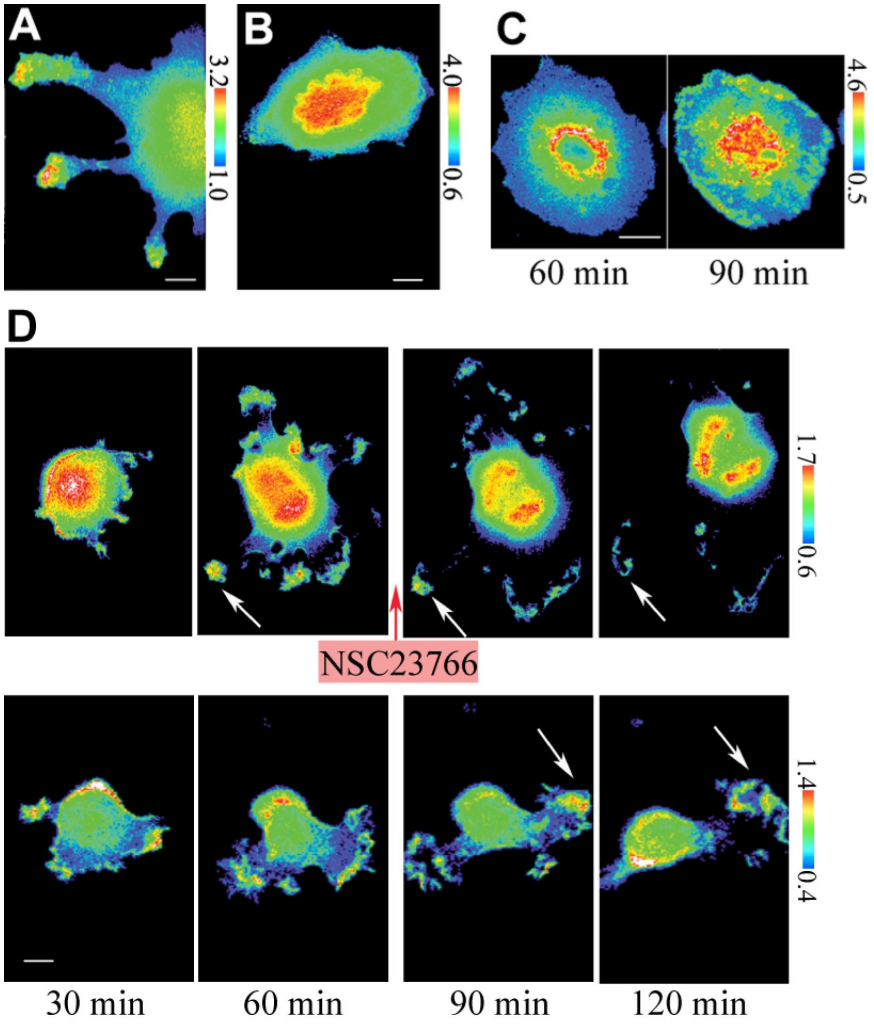

E Cells with high Rac activity at the edge

Schwannoma cells	14/16 (87.5%)
Normal Schwann cells	0/12 (0%)
Schwannoma cells: NSC23766 treatment	2/7 (28.6%)
Schwannoma cells: NSC23766 washout	8/11 (72.7%)

Figure 2. The distribution of Rac activity in schwannoma cells/normal Schwann cells. ***A***, ***B***, YFP/CFP ratio images of cells expressing Raichu-Rac1–1011x were acquired 60 min after plating. High FRET efficiency was observed at the edges in schwannoma cells (***A***) but not in normal Schwann cells (***B***). Images are representative of 16 (***A***) or 12 (***B***) independent cells. ***C***, Raichu-Rac1–1011x was verified by monitoring the efficiency and the reversibility of NSC23766 on Rac activity. Schwannoma cells were pretreated with NSC23766 and then plated after washing out the inhibitor. High FRET efficiency of Raichu-Rac1–1011x at the edge was suppressed by NSC23766 pretreatment at 60 min and was reversed at 90 min. Images are representative of 18 cells. ***D***, Raichu-Rac1–1011x was verified by monitoring the efficacy of NSC23766 to suppress Rac activity. Schwannoma cells were treated with (top) or without (bottom) NSC23766 after 60 min of plating. Minutes indicate time after plating. High FRET efficiencies at the cell edges were suppressed within 60 min after adding the inhibitor (arrows in top), which remained high without the inhibitor (arrows in bottom). Images are representative of four independent measurements. ***E***, YFP/CFP ratio images of cells in conditions described in ***A–C*** were acquired randomly. Cells with high FRET efficiency at the edges were counted. Scale bars, 10 μm.

These biochemical and cell biological results show the efficacy and specificity of NSC23766 in Schwann cells and schwannoma cells, allowing us to use this compound to probe a requirement for regulated GTP-Rac in Schwann cell–neuron interaction.

Rac is activated at a specific region in schwannoma cells

To monitor spatiotemporal activity of Rac in cells, we used a FRET probe, Raichu-Rac1–1011x (Itoh et al., 2002). Raichu-Rac1–1011x is a fusion protein of Rac1 and its effector PAK with

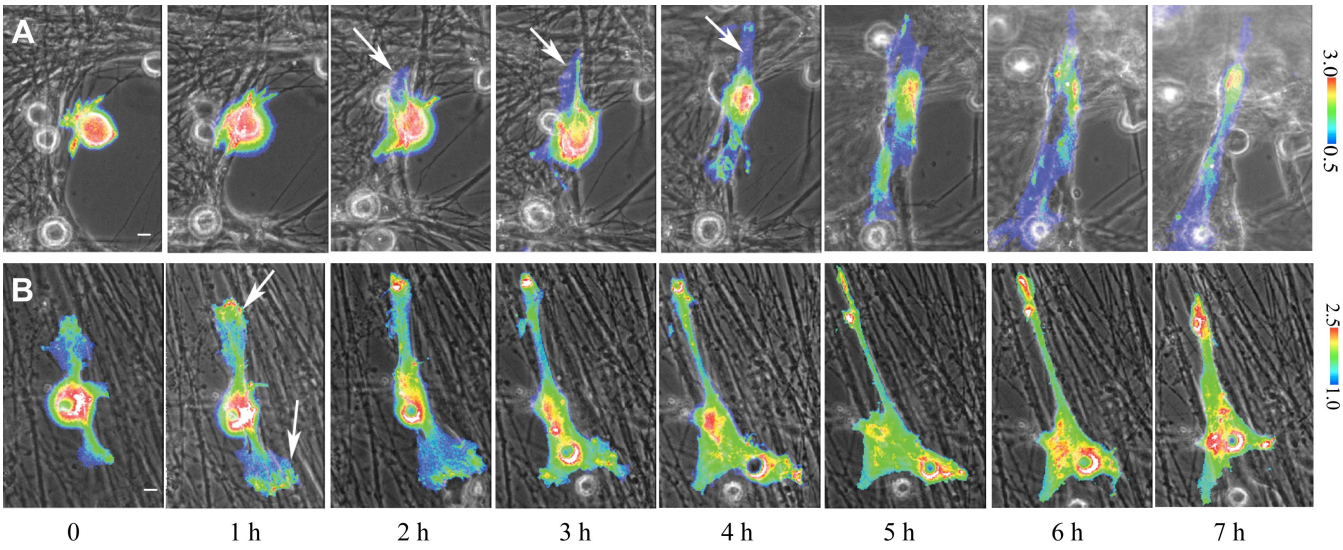

Figure 3. Kinetics of Rac activity in normal Schwann cells/schwannoma cells during neuronal interaction. ***A***, ***B***, Overlay images of phase-contrast images and YFP/CFP ratio images during Schwann cell–neuron coculture. Normal human Schwann cells (***A***) and schwannoma cells (***B***) expressing Raichu-Rac1–1011x probe were cocultured with rat DRG neurons. In normal Schwann cells, Rac was inactive at the elongating processes (arrows in ***A***), whereas in schwannoma cells, it was highly active at the edge of the cells (arrows in ***B***; images are representative of 2 independent measurements). Hours indicate time after interaction. Scale bars, 10 μm.

CFP and YFP on each terminus. When Rac1 is activated, it binds to PAK so the fusion protein folds. This conformational change brings CFP into proximity to YFP, resulting in energy transfer of CFP emission energy to YFP excitation energy (Itoh et al., 2002). This energy transfer is measured as FRET efficiency. Here we used YFP/CFP ratio to represent FRET efficiency.

First, we monitored GTP-Rac in Schwann cells or schwannoma cells. YFP/CFP images of cells expressing Raichu-Rac1–1011x probe were acquired 60 min after plating. Here and if not specified, poly-D-lysine-coated cover glass was used as a substrate and cells were maintained in the presence of 10% serum. Schwannoma cells showed high Rac activity at the edge of the cells (Fig. 2*A*), the region consistent with the actin accumulation in ruffling membranes (Fig. 1*C*), but normal Schwann cells did not (Fig. 2*B*). Fourteen of 16 and 0 of 12 cells showed high Rac activity at the edges in schwannoma cells and normal Schwann cells, respectively (Fig. 2*E*). When another FRET probe, Racichu-RhoA-1237x, which consists of a fusion protein of RhoA and its effector protein kinase novel, that monitors RhoA activity on the same principle (Yoshizaki et al., 2003) was used, high FRET efficiency at the edge of schwannoma cells was not shown. Racichu-RhoA-1237x showed a fiber-like distribution of high FRET efficiency in Schwann cells and schwannoma cells (data not shown). This indicated that the high FRET efficiency observed at the edges of schwannoma cells was specific to Racichu-Rac1–1011x.

To confirm that Racichu-Rac1–1011x was monitoring Rac activity in the FRET assay, we added NSC23776 Rac inhibitor to schwannoma cells before or during the observation period. When schwannoma cells were pretreated with NSC23766 in cell suspension and then plated for 60 min after washing out the inhibitor, high FRET efficiency at the periphery of the cells was suppressed (Fig. 2*C*, left). This suppression was reversible; within 90 min after washing out the inhibitor, the FRET efficiency increased, especially at the edges of cells (Fig. 2*C*, right). When schwannoma cells were both pretreated and plated in the inhibitor, the FRET efficiency remained low during the same time course (data not shown). With continuous treatment of NSC23766, only 28.6% of the cells showed high FRET efficiency at the edge, whereas when the inhibitor was washed out, 72.7% of the cells did (Fig. 2*E*). We also added the inhibitor to schwannoma cells after plating. The FRET efficiency of Raichu-Rac1–1011x probe was reduced within 60 min after adding NSC23766 (Fig. 2*D*, top). Without NSC23766, high FRET efficiency was continuously monitored at the edges of the cell during the same time course (Fig. 2*D*, bottom). We tested four individual cells, and all cells showed reduction of FRET efficiency within 3 h after adding the inhibitor. The same experiment was performed on schwannoma cells expressing Racichu-RhoA-1237x. The FRET efficiency of Raichu-RhoA-1237x did not decrease after the addition of NSC23766 (data not shown). Thus, the FRET efficiency attributable to Rachu-Rac1–1011x specifically corresponded to both the efficiency and the reversibility of NSC23766. We concluded that Rachu-Rac1–1011x was a suitable tool to monitor Rac activity in our system. Notably, schwannoma cells but not normal Schwann cells showed high Rac activity at the edge of the cells.

Kinetics of Rac activity during neuronal interaction differs between Schwann cells and schwannoma cells

The aim of this study was to explore Rac activity in Schwann cell–neuron interaction and to explore the relevance of GTP-Rac to the abnormalities of schwannoma cells. We used Raichu-Rac1–1011x FRET probe to analyze the spatiotemporal specificity of Rac activities in Schwann cells during Schwann cell–neurite interaction. Normal human Schwann cells or schwannoma cells expressing Raichu-Rac1–1011x were plated onto a neurite network substrate established from dissociated rat DRG neurons. Under these conditions, normal Schwann cells first attach to neurites and then elongate processes over the course of several hours (Wanner and Wood, 2002). Imaging was initiated 60 min after addition of cells to cultured neurons. In normal human Schwann cells, GTP-Rac was high in numerous small processes at initial contact with the neurites. Within 3 h, Schwann cell processes began to elongate along neurites and showed low GTP-Rac (Fig. 3*A*, arrows). Nine cells at initial contact and four cells starting to elongate processes were examined. In each cell, the same spatiotemporal sequence was observed.

Schwannoma cells showed a striking difference from normal

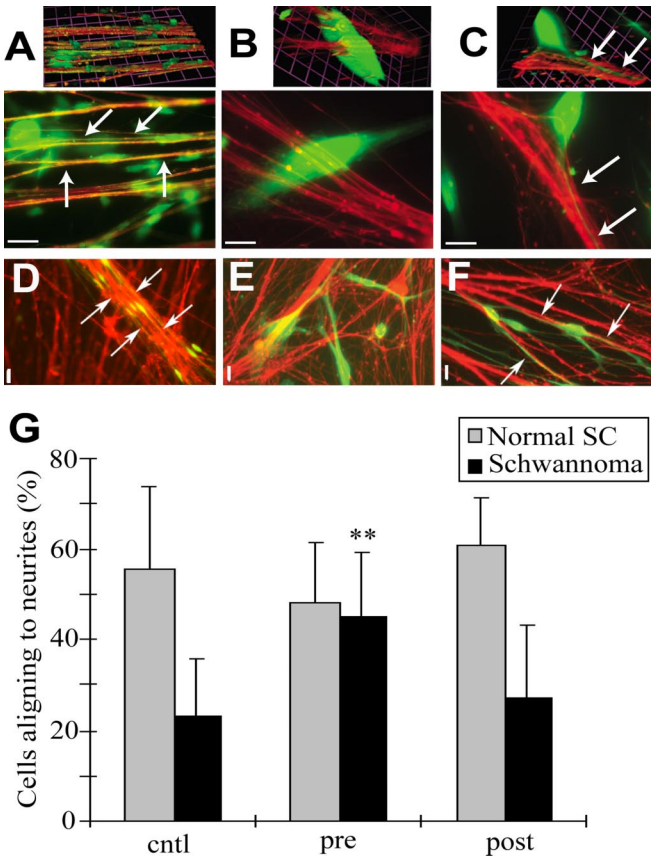

Figure 4. Inhibition of Rac restored the ability to interact with neurites to schwannoma cells. ***A–F***, Normal human Schwann cells (***A***, ***D***) and schwannoma cells (***B***, ***C***, ***E***, ***F***) (green), with (***C***, ***F***) or without (***A***, ***B***, ***D***, ***E***) NSC23766 pretreatment were cocultured with rat DRG neurons (red). High-magnification (63×) images (***A–C***; top) with three-dimensional images (***A–C***; top) and low-magnification (10×) images (***D–F***) are shown. Normally, Schwann cells align their cell bodies and processes with neurites during neuronal interaction (arrows in ***A***, ***D***). Schwannoma cells did not elongate processes along neurites (***B***, ***E***). Schwannoma cells with NSC23766 pretreatment elongated their processes along neurites (arrows in ***C***, ***F***). Images are representative of a panel of cells in each condition. Scale bars: ***A–C***, 10 μm; ***D–F***, 20 μm. ***G***, Normal Schwann cells (SC) and schwannoma cells with processes aligning with neurites were quantified. Cells were treated with NSC23766 before coculture (pre) or from 3 h after starting the coculture (post). Neuronal alignment was restored to schwannoma cells by NSC23766 pretreatment. Error bars represent mean ± SD. $^{**}p < 0.005$ (Student's *t* test).

Schwann cells. They did not suppress Rac activity during the time course (Fig. 3*B*). Notably, there were multiple regions containing high GTP-Rac in distal cell membrane (Fig. 3*B*, arrows), which had a similar appearance to highly active regions of Rac shown in ruffling cells (Fig. 2*A*). When normal Schwann cells and schwannoma cells were plated onto a laminin substrate, which enhances membrane spreading of Schwann cells without neurons, the same difference was shown; Rac was first activated and then became suppressed in normal Schwann cells during membrane spreading, whereas in schwannoma cells, it was continuously highly active (data not shown). This suggested that the difference in GTP-Rac between normal Schwann cells (Fig. 3*A*) and schwannoma cells (Fig. 3*B*) during neuronal contact were caused not by the neurons but by endogenous mechanisms of the Schwann cells.

Suppression of Rac improves alignment of schwannoma cells to neurites

Because GTP-Rac is sustained in schwannoma cells during neuronal contact, we hypothesized that suppression of GTP-Rac might enable process elongation of schwannoma cells on neurites. We downregulated GTP-Rac in normal Schwann cells and schwannoma cells using NSC23766 and measured the percentage of Schwann cells with processes aligned along neurites. When normal human Schwann cells are cocultured with rat DRG neurons for 24 h, a majority (55.7%) align their processes with neurites (Fig. 4*A*,*D*). Correlating with their lack of interaction with axons within tumors, schwannoma cells showed significantly less alignment (23.0%) (Fig. 4*B*,*E*). When schwannoma cells were treated with NSC23766 before coculture, spindle morphology was restored, and cells elongated processes along the neurites (44.8%) (Fig. 4*C*,*F*).

To address whether suppression of GTP-Rac is required in Schwann cells before or during process elongation, we treated cells with NSC23766 before or 3 h after initiating the coculture. Pretreated cells were washed before addition to neurons and plated without the drug. Pretreatment with NSC23766 did not significantly affect normal Schwann cell interaction with neurites (Fig. 4*G*). This could be explained by reversibility of NSC23766, or, alternatively, transient Rac activation in normal Schwann cells may not be required for process elongation. Pretreatment of schwannoma cells with NSC23766 significantly restored neuronal alignment (Fig. 4*C*,*F*,*G*), suggesting that high GTP-Rac precludes early cell–cell interaction and/or later process extension and alignment. To discriminate these alternatives, the inhibitor was added 3 h after starting the coculture. There was no significant effect on normal Schwann cells or on schwannoma cells (Fig. 4*G*). These results suggest that normal regulation of Rac is required at an early time point in Schwann cell–neurite contact, likely early cell–cell interaction and/or early process extension, and that, once the membranes of schwannoma cells are spread (Fig. 4*B*,*E*), functional processes do not emerge even with NSC23766 treatment.

Discussion

How schwannoma cells accomplish neuronal alignment after washout of NSC23766 remains to be revealed. Extrinsic neuronal factors may continue to suppress GTP-Rac. Alternatively, intrinsic Schwann cell signaling may be involved. For example, other small GTPases may suppress Rac after initial process elongation; indeed, Rho activity has been implicated in dynamic movement of Schwann cell tips and myelination, whereas Rac/Cdc42 has been implicated in migration (Gatto et al., 2003; Melendez-Vasquez et al., 2004; Yamauchi et al., 2004). Alternatively, regulation of Rac may no longer be required once process elongation is started. In either case, the efficacy of NSC23766 in schwannoma cells suggests the plausible therapeutic strategy of targeting Rac in *NF2*-related disease. The recent demonstration that NSC23766 can be used *in vivo* supports this direction (Cancelas et al., 2005). In summary, we have shown specific deregulation in both quantity and spatial distribution of GTP-Rac in human schwannoma cells when compared with Schwann cells. Furthermore, we have shown that this deregulation appears to at least in part account for abnormalities of cell morphology and function in that its specific suppression leads to normalization in both arenas. Rac inhibition should be considered in the pharmacological treatment of human Schwann cell tumors.

References

Bashour AM, Meng JJ, Ip W, MacCollin M, Ratner N (2002) The neurofibromatosis type 2 gene product, merlin, reverses the F-actin cytoskeletal defects in primary human Schwannoma cells. Mol Cell Biol 22:1150–1157.

Cancelas JA, Lee AW, Prabhakar R, Stringer KF, Zheng Y, Williams DA

(2005) Rac GTPases differentially integrate signals regulating hematopoietic stem cell localization. Nat Med 11:886–891.

Fernandez-Valle C, Gorman D, Gomez AM, Bunge MB (1997) Actin plays a role in both changes in cell shape and gene-expression associated with Schwann cell myelination. J Neurosci 17:241–250.

Gao Y, Dickerson JB, Guo F, Zheng J, Zheng Y (2004) Rational design and characterization of a Rac GTPase-specific small molecule inhibitor. Proc Natl Acad Sci USA 101:7618–7623.

Gatto CL, Walker BJ, Lambert S (2003) Local ERM activation and dynamic growth cones at Schwann cell tips implicated in efficient formation of nodes of Ranvier. J Cell Biol 162:489–498.

Hall A (1998) Rho GTPases and the actin cytoskeleton. Science 279:509–514.

Itoh RE, Kurokawa K, Ohba Y, Yoshizaki H, Mochizuki N, Matsuda M (2002) Activation of rac and cdc42 video imaged by fluorescent resonance energy transfer-based single-molecule probes in the membrane of living cells. Mol Cell Biol 22:6582–6591.

Kaempchen K, Mielke K, Utermark T, Langmesser S, Hanemann CO (2003) Upregulation of the Rac1/JNK signaling pathway in primary human schwannoma cells. Hum Mol Genet 12:1211–1221.

Kissil JL, Wilker EW, Johnson KC, Eckman MS, Yaffe MB, Jacks T (2003) Merlin, the product of the Nf2 tumor suppressor gene, is an inhibitor of the p21-activated kinase, Pak1. Mol Cell 12:841–849.

Maeda M, Matsui T, Imamura M, Tsukita S, Tsukita S (1999) Expression level, subcellular distribution and rho-GDI binding affinity of merlin in comparison with Ezrin/Radixin/Moesin proteins. Oncogene 18:4788–4797.

Melendez-Vasquez CV, Einheber S, Salzer JL (2004) Rho kinase regulates Schwann cell myelination and formation of associated axonal domains. J Neurosci 24:3953–3963.

Okada T, Lopez-Lago M, Giancotti FG (2005) Merlin/NF-2 mediates contact inhibition of growth by suppressing recruitment of Rac to the plasma membrane. J Cell Biol 171:361–371.

Parysek LM, Goldman RD (1987) Characterization of intermediate filaments in PC12 cells. J Neurosci 7:781–791.

Pelton PD, Sherman LS, Rizvi TA, Marchionni MA, Wood P, Friedman RA, Ratner N (1998) Ruffling membrane, stress fiber, cell spreading and proliferation abnormalities in human Schwannoma cells. Oncogene 17:2195–2209.

Ridley AJ, Paterson HF, Johnston CL, Diekmann D, Hall A (1992) The small GTP-binding protein rac regulates growth factor-induced membrane ruffling. Cell 70:401–410.

Shaw RJ, Paez JG, Curto M, Yaktine A, Pruitt WM, Saotome I, O'Bryan JP, Gupta V, Ratner N, Der CJ, Jacks T, McClatchey AI (2001) The Nf2 tumor suppressor, merlin, functions in Rac-dependent signaling. Dev Cell 1:63–72.

Vabnick I, Novakovic SD, Levinson SR, Schachner M, Shrager P (1996) The clustering of axonal sodium channels during development of the peripheral nervous system. J Neurosci 16:4914–4922.

Wanner IB, Wood PM (2002) N-cadherin mediates axon-aligned process growth and cell-cell interaction in rat Schwann cells. J Neurosci 15:4066–4079.

Xiao GH, Gallagher R, Shetler J, Skele K, Altomare DA, Pestell RG, Jhanwar S, Testa JR (2005) The NF2 tumor suppressor gene product, merlin, inhibits cell proliferation and cell cycle progression by repressing cyclin D1 expression. Mol Cell Biol 25:2384–2394.

Yamauchi J, Chan JR, Shooter EM (2004) Neurotrophins regulate Schwann cell migration by activating divergent signaling pathways dependent on Rho GTPases. Proc Natl Acad Sci USA 101:8774–8779.

Yoshizaki H, Ohba Y, Kurokawa K, Itoh RE, Nakamura T, Mochizuki N, Nagashima K, Matsuda M (2003) Activity of Rho-family GTPases during cell division as visualized with FRET-based probes. J Cell Biol 162:223–232.